

Influence functional of many-body systems: temporal entanglement and matrix-product state representation

Michael Sonner,^{1,*} Alessio Lerose,^{1,*} and Dmitry A. Abanin¹

¹*Department of Theoretical Physics, University of Geneva,
Quai Ernest-Ansermet 30, 1205 Geneva, Switzerland*

(Dated: March 26, 2021)

Feynman-Vernon influence functional (IF) was originally introduced to describe the effect of a quantum environment on the dynamics of an open quantum system. We apply the IF approach to describe quantum many-body dynamics in isolated spin systems, viewing the system as an environment for its local subsystems. While the IF can be computed exactly only in certain many-body models, it generally satisfies a self-consistency equation, provided the system, or an ensemble of systems, are translationally invariant. We view the IF as a fictitious wavefunction in the temporal domain, and approximate it using matrix-product states (MPS). This approach is efficient provided the *temporal entanglement* of the IF is sufficiently low. We illustrate the broad applicability of the IF approach by analyzing several models that exhibit a range of dynamical behaviors, from thermalizing to many-body localized. In particular, we study the non-equilibrium dynamics in the quantum Ising model in both Floquet and Hamiltonian settings. We find that temporal entanglement entropy may be significantly lower compared to the spatial entanglement and analyze the IF in the continuous-time limit. We simulate the thermodynamic-limit evolution of local observables in various regimes, including the relaxation of impurities embedded in an infinite-temperature chain, and the long-lived oscillatory dynamics of the magnetization associated with the confinement of excitations. Furthermore, by incorporating disorder-averaging into the formalism, we analyze discrete time-crystalline response using the IF of a bond-disordered kicked Ising chain. In this case, we find that the temporal entanglement entropy scales logarithmically with evolution time. The IF approach offers a new lens on many-body non-equilibrium phenomena, both in ergodic and non-ergodic regimes, connecting the theory of open quantum systems theory to quantum statistical physics.

I. INTRODUCTION

The problem of a quantum system interacting with an environment has played an important role since the early days of quantum mechanics [1]. Describing dynamics of such *open quantum systems* is essential for understanding diverse phenomena including the process of quantum measurement, transport in nanostructures, and thermalization [2].

It is an extremely challenging task to describe sufficiently complex, realistic environments exactly. Therefore much work focused on studying simplified models of environments, and on developing approximations for open system dynamics. A model that played a special role is that of an environment made of harmonic oscillators [3] which do not interact among themselves. Interestingly, the dynamics of a seemingly simple open quantum system – a two-level system interacting with such a bosonic environment (or a bath) – exhibits a rich variety of regimes, depending on the spectral density of the oscillators [4].

More recently, experimental advances have enabled realization of many-body quantum systems which are well isolated from an external environment [5, 6]. Such setups have brought into focus the problem of highly non-equilibrium dynamics in *closed* many-body systems. Var-

ious universality classes, distinguished by their drastically different dynamical behavior, have been discovered.

The most common class is that of thermalizing, or ergodic dynamics: starting from generic initial states, local subsystems reach an effectively thermal state under unitary dynamics [7]. Remarkably, ergodicity can be broken by disorder-induced many-body localization (MBL) [8–10], as first foreseen by Anderson in the paper reporting discovery of single-particle localization [11]. Persistence of MBL in periodically driven (Floquet) systems [12–15] has opened the door to novel non-equilibrium phases such as discrete time crystals [16, 17] and anomalous Floquet insulators [18]. Much attention has also focused on investigating dynamics in integrable one-dimensional systems, which at long times relax to a generalized Gibbs ensemble [19], and on weak ergodicity breaking mechanisms such as quantum scars [20].

At an intuitive level, the character of the system’s dynamics is determined by its properties as a quantum environment. An ergodic system acts as a “good” thermal bath for its subsystems, while MBL and other non-ergodic systems fail to do so. This observation links the dynamics of a many-body system to that of an open quantum system; however, the environment is now itself a complex interacting system, rather than a set of non-interacting harmonic oscillators.

The ability of a many-body system to act as a thermal bath has been characterized using a number of eigenstate and dynamical probes [7, 9, 10]. The eigenstate thermalization hypothesis (ETH) [21, 22], as well as its

* These two authors contributed equally to this work

breakdown in MBL systems provide a particularly useful tool. One may also directly study the dynamics of physical observables following a quantum quench using numerical techniques such as exact diagonalization and tensor networks [23, 24], and verify whether they settle to thermal values. The quantum quench setup is routinely employed experimentally in different platforms, including cold atoms, trapped ions, and superconducting qubits.

In this paper, building on very recent ideas [25, 26] and earlier related work [27], we employ the Feynman-Vernon influence functional to analyze the problem of quantum dynamics and characterize the properties of a many-body system as an environment. The influence functional (IF) for an open quantum system is obtained by performing the Keldysh path integral over the environment degrees of freedom $\{q_j(\tau), \bar{q}_j(\tau)\}$, subject to a time-dependent trajectory of the system $Q(\tau), \bar{Q}(\tau)$ (here and below each trajectory has a forward and a backward part, and coordinates without/with a bar parametrize the former/latter). The idea of this approach is illustrated in Fig. 1a: the effect of the environment is completely described by the IF $\mathcal{I}[Q(\tau), \bar{Q}(\tau)]$, which weighs the trajectories of the system. The explicit expression for the IF, available for certain simplified models such as a bath of harmonic oscillators, has provided a starting point for describing a two-level system subject to dissipation [4].

The approach proposed in Ref. [25] is based on the observation that the IF of a spatially homogeneous many-body system, while difficult to compute directly, satisfies a self-consistency equation. In the tensor-network language, this equation amounts to finding an eigenvector of the dual transfer matrix arising in the path-integral description of the system's dynamics [27], as schematically illustrated in Fig. 1b,c. This eigenvector can be efficiently sought in the form of a matrix-product state (MPS), provided its *temporal entanglement* remains low. This is analogous to how MPS-based algorithms such as the density matrix renormalization group rely on the spatial entanglement of ground states being low [23]. However, while the latter is guaranteed by rigorous results concerning area-law entanglement scaling in gapped systems, relatively little is known about the scaling of temporal entanglement.

It was appreciated early on [28] that for certain dynamical problems the approaches based on transverse contractions of the time-evolution tensor network be computationally more favorable compared to the conventional methods such as the time-evolving block decimation (TEBD). The recent work [25], which considered periodically driven (Floquet) systems, found that in a family of thermalizing models, including so-called dual-unitary circuits [29–31], the discrete-time IF – or influence matrix (IM) – can be found exactly and has vanishing temporal entanglement. Furthermore, Ref. [32] found a different exact MPS solution for an integrable quantum cellular automaton. The IF approach to a Floquet-MBL model was shown to be efficient as well [33]. In a different

direction, Refs. [26, 34, 35] proposed a tensor-network-based compression of the IF of baths of noninteracting particles.

In this paper, we extend the IF approach and demonstrate its utility for several classes of non-equilibrium problems of current interest, both in ergodic and non-ergodic regimes. We first employ it to describe thermalization dynamics in Floquet and Hamiltonian many-body systems. Focusing on spin-1/2 chains, we apply the IF formalism to compute the behavior of dynamical correlators in an infinite-temperature ensemble. Furthermore, we analyze the time-dependent observables following a quantum quench starting from simple pure initial states. In particular, we simulate the long-lived oscillations of local observables that arise due to confinement of excitations in the quantum Ising chain in a tilted field [36–39].

In a different direction, below we adapt the IF approach to analyze the dynamics of non-equilibrium, non-ergodic phases. We focus on a one-dimensional discrete time-crystal (DTC) enabled by disorder-induced MBL. Our approach allows us to perform exact averaging over the disordered spin-spin couplings (see below). We then consider the self-consistency equation for the disordered-averaged IF, and solve it using an MPS representation.

In this paper we will be particularly interested in the scaling of temporal entanglement (TE) entropy with the evolution time. We find that in all problems considered, TE remains relatively low up to sizable evolution times, which indicates efficiency of the MPS representation of the IF. Furthermore, we investigate the behavior of TE in Hamiltonian systems as the continuum limit is taken by decreasing the time step in the Trotterized evolution operator. Surprisingly, TE entropy decreases to zero in the limit of vanishing time steps; however, as we argue below, small singular values may not always be truncated to faithfully approximate the IF of a Hamiltonian system.

The rest of the paper is organized as follows. In the subsequent Section II, we introduce the IF approach for both Floquet and Hamiltonian dynamics. We also discuss the MPS representation and the method we use to numerically compute the IF. Subsequently, in Section III we analyze thermalization dynamics in a (non-integrable) quantum Ising model, presenting results for quenches from different initial ensembles/states. Both Floquet and Hamiltonian dynamics will be considered. Further, in Section IV we turn to non-ergodic dynamics and discuss how to incorporate disorder-averaging into the IF formalism, considering discrete time crystal (DTC) as an application. We conclude in Section V by discussing future directions and potential of the IF approach to quantum many-body dynamics and open quantum systems.

II. INFLUENCE FUNCTIONAL FOR MANY-BODY DYNAMICS

We start our analysis by formulating the influence functional approach to describing dynamics of a many-

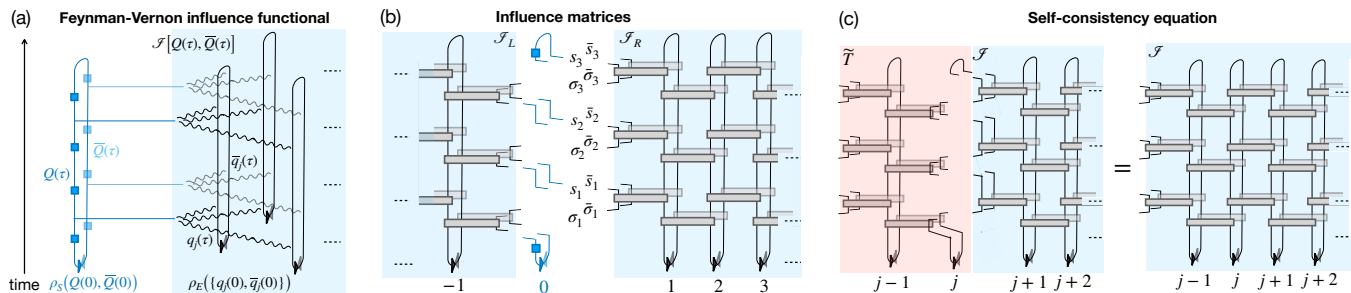


Figure 1. a) Idea of the Feynman-Vernon influence functional for a quantum system interacting with a bath, which consists of non-interacting harmonic oscillators. Considering the time evolution in the Keldysh path integral representation, the bath degrees of freedom $\{q_j(\tau), \bar{q}_j(\tau)\}$ are integrated out. This yields a contribution $\mathcal{I}[Q(\tau), \bar{Q}(\tau)]$ in the path integral over the system coordinates only, which is the influence functional. b) A tensor network describing evolution of a spin chain, in the discrete path integral representation. Time runs upwards and the foreground (background) represents the forward (backward) branch of time evolution. Contraction of the parts of the network contained in the blue-shaded boxes defines the left and right influence matrices – tensors acting on the space of trajectories of spin $j = 0$. For the case of Hamiltonian evolution, when the tensor network represents a discretization of the continuous time evolution, the influence matrices approximate the corresponding continuous-time influence functionals. c) The influence functional of a homogeneous spin system is an eigenvector of the dual transfer-matrix represented by the red-shaded box; equivalently, it satisfies a linear self-consistency equation (7).

body system. Throughout the paper, we focus on one-dimensional lattice systems of spins with local Hilbert space dimension q subject to local two-body interactions. We note that the extensions to bosons/fermions, longer-range k -body interactions, and to higher-dimensional systems are straightforward. We consider models in which the time evolution can be represented by a general “brick-wall” quantum circuit (Fig. 1b). This class includes Floquet models, and trotterized Hamiltonian evolution. We note that Ref. [25] introduced the IF approach for a narrower class of Floquet models.

The central idea of the approach is summarized in Fig. 1b,c. The evolution operator over one period of the brick-wall circuit is given by:

$$U = U_e U_o, \quad U_o = \prod_j U_{2j-1, 2j}, \quad U_e = \prod_j U_{2j, 2j+1}, \quad (1)$$

where the two operators correspond to odd and even layers of the quantum circuit. The two-body evolution operators (unitary gates) in the above expression define the model in the case of Floquet dynamics. For the case of Hamiltonian evolution, generated by a two-body local Hamiltonian,

$$H = \sum_i H_{i, i+1}, \quad (2)$$

the gates are obtained by trotterizing the time evolution, with a time step $\epsilon \rightarrow 0$:

$$U_{i, i+1} = e^{-iH_{i, i+1}\epsilon}. \quad (3)$$

The physical evolution time t in the Hamiltonian case is the product of the time step ϵ and the number of time steps T in the tensor network in Fig. 1b, i.e., $t = T\epsilon$. We note that the brick-wall quantum circuit can also be used to encode higher-order Trotter schemes; here for simplicity we will consider only the lowest-order scheme.

The time-evolved density matrix of the system after T steps of evolution is related to the initial state density matrix ρ^0 as follows:

$$\rho^T = U^T \rho^0 U^{+T}. \quad (4)$$

For simplicity, we will consider initial density matrices which can be represented as a tensor product of individual spin density matrices, i.e.,

$$\rho^0 = \bigotimes_j \rho_j^0. \quad (5)$$

Rewritten via a discrete path integral over intermediate configurations of the system, the time evolution in Eq. (4) can be represented by a tensor network, as illustrated in Fig. 1b. We denote the forward and backward trajectory of spin j by $\sigma_j^\tau, \bar{\sigma}_j^\tau, s_j^\tau, \bar{s}_j^\tau$, as shown in the Figure. The gates acting in the forward part of the network are $U_{j, j+1}$ and the ones in the backward part of the network are $U_{j, j+1}^*$.

We will be interested in describing the evolution of a sufficiently small subsystem, e.g. a single spin $j = 0$. The dynamics can be characterized by correlation functions of the form

$$\langle \hat{O}_0(T) \hat{O}_0(0) \rangle, \quad (6)$$

where \hat{O}_0 is an operator representing a local observable at site $j = 0$, see Fig. 1b. To calculate such correlators we begin by tracing out the environment degrees of freedom, i.e., the other spins; the spins with $j > 0$ can be viewed as a “right” environment, and the ones with $j < 0$ as a “left” environment. This procedure yields right and left influence matrices $\mathcal{I}_{R(L)}$, which are formally introduced by contracting tensor networks contained in the blue-shaded boxes in Fig. 1b, with a boundary defined

by spin $j = 0$ trajectory; in this contraction, the summation over all final states of the spins in the environment is carried out. We can now calculate any correlator of the form Eq. (6) by contracting the IMs with a tensor network for evolution of spin $j = 0$, with operators \hat{O}_0 inserted at $\tau = 0, T$. In the Hamiltonian case, the IMs approximate the corresponding continuous-time IFs as $\epsilon \rightarrow 0$. (In the following we will often use the names IM and IF interchangeably.)

In certain cases, which include dual-unitary circuits/perfect dephasers [25, 29–31] and certain integrable systems [32, 40], the contraction of the tensor network that defines the IF can be carried out analytically. Generally, the IF for an environment with two additional spins can be obtained from the previous IF by applying one vertical slice of the tensor network in Fig. 1c (red shaded box). These vertical slices define the *dual transfer matrices* [27], which act on the q^{4T} -dimensional space of single-spin trajectories. As discussed below, for certain systems contracting the tensor network in the space direction using dual transfer matrices proves advantageous compared to the standard contraction in time direction.

In translationally invariant systems, the dual transfer matrix \tilde{T} is the same at every step. Notice that the strict light cone in our model means that the IF that describes evolution over time T can depend at most on the motion of closest $2T$ spins. Hence the IF of a homogeneous system is a unique eigenvector of \tilde{T} with an eigenvalue 1. The eigenvalue equation for the right IF

$$\tilde{T}|\mathcal{I}\rangle = |\mathcal{I}\rangle, \quad (7)$$

(where we omitted the subscript R for simplicity) has a simple physical interpretation: it can be viewed as a *self-consistency equation* for the IF. In essence, a spin evolving under the influence of the right environment, exerts the same influence on its left neighbor. The left influence functional clearly satisfies an analogous equation with a slightly modified transfer matrix.

We note that this approach can be extended to describe ensembles of disordered models with spatially uncorrelated, translationally-invariant distribution: in that case, the transfer matrix in Eq. (7) is disorder-averaged, and its eigenvector corresponds to an IF of a disorder-averaged environment. In Ref. [33], a particular Floquet-MBL model with on-site disorder fields was considered (see also Refs. [41–43]). Below in Section IV we will discuss a generalization of the method to a model with disordered two-body interactions, which exhibits discrete time crystal behavior.

A promising approach to solving the self-consistency equation (7) is based on approximating the influence matrix by an MPS with a fixed bond dimension [25, 27, 28], similarly to conventional techniques for two-dimensional systems [44]. This approach is expected to be efficient when TE entropy is low. In that case, the IF formulation may allow one to analyze time-dependent correlation functions which are out of reach of standard methods such as TEBD, exact diagonalization, etc.

Interestingly, temporal entanglement can be low in different dynamical regimes. A striking example is provided by perfect-dephaser Floquet circuits: for an infinite-temperature initial density matrix and certain pure initial states in MPS form, the IF is a product state with zero TE [25, 31]; in this case, the environment effectively dephases local spins at every step of Floquet evolution. TE remains low in the vicinity of such solvable points, which ensures the efficiency of the MPS representation. Furthermore, the TE was found to be low up to long times in certain non-integrable Hamiltonian models [28, 45], and in proximity to integrability [40]. Ref. [33] further demonstrated that the approach remains efficient in the ergodicity-breaking Floquet-MBL phase, thanks to slow, sub-linear scaling of TE of the disorder-averaged IF. Despite these results, the full potential of the IF-based approach to describe quantum dynamics remains to be investigated; the key open question concerns the scaling of TE with the evolution time and the formulation of suitable numerical algorithms to approximate it.

In what follows, we will analyze several Hamiltonian and Floquet models, both in the ergodic and non-ergodic regimes. We will compute dynamical correlation functions using the IF approach for both mixed and pure initial states of the system. We will also investigate the scaling of TE, and its dependence on the system's parameters, and on the time evolution step ϵ , for the case of Hamiltonian dynamics.

III. THERMALIZING DYNAMICS IN FLOQUET AND HAMILTONIAN SYSTEMS

In this Section, we will study thermalization dynamics in non-disordered Floquet and Hamiltonian models in different setups using the IF approach. We will consider relaxation of observables in a chaotic system initialized in an infinite-temperature ensemble, both for a spin that is part of the system, and for an impurity embedded in a many-body environment. Further, quench dynamics from a pure initial state in a model with confined excitations will be studied. For all examples considered, we will investigate the behavior of TE entropy with evolution time.

A. Floquet dynamics

We start by illustrating the use of the method for Floquet systems. As an example of a thermalizing Floquet model, we choose the kicked Ising model for spins-1/2, which has been extensively studied in the literature [29, 30, 46]. The Floquet operator of this model is given by:

$$U = e^{-ig \sum_j \sigma_j^x} e^{-iJ \sum_j \sigma_j^z \sigma_{j+1}^z - ih \sum_j \sigma_j^z}, \quad (8)$$

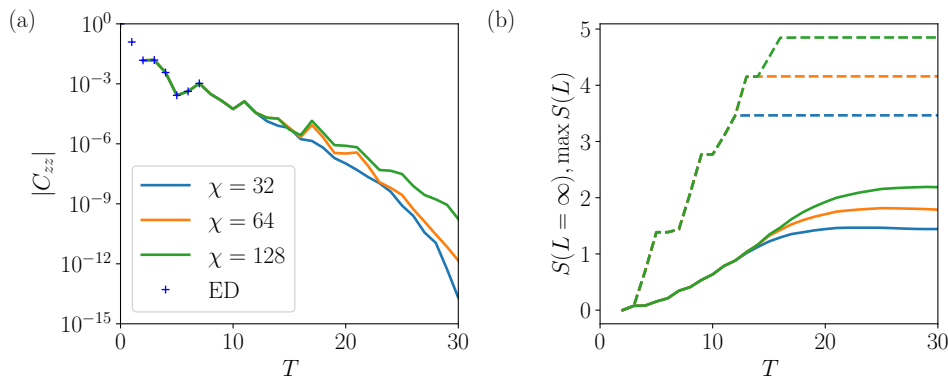


Figure 2. Simulation of the kicked Ising model Eq.(8) with parameters $J = 0.8, g = 0.7236, h = 0.6472$ [46] for an infinite-temperature initial state. *Left*: Autocorrelation function of the σ^z operator as a function of time. Exponential relaxation signals chaotic dynamics. The blue crosses correspond to exact diagonalization results, which coincide with the MPS calculations. The results are well converged up to time $T \approx 20$. *Right*: Temporal entanglement entropy as a function of evolution time for different bond dimensions. Dashed lines are maximal entanglement entropies which are encountered during iteration process starting from open boundary IF. Starting from the PD IF, the entropy of the final IF is also the maximal entropy (solid lines). This illustrates the importance of the choice of the initial IF in the context of the iterative MPS method.

where σ_j^α , $\alpha = x, y, z$ are standard spin-1/2 Pauli operators. Depending on the values of parameters J, g, h , the model displays a rich variety of dynamical behavior. For $h = 0$, it can be mapped onto a free-fermion model using a Jordan-Wigner transformation, and is therefore integrable. In this case, it can be shown that the IF obeys an area-law temporal entanglement, even in the limit of very long evolution times, $T \rightarrow \infty$ [40].

Furthermore, the model has special properties at the self-dual points $|J| = |g| = \pi/4$ [29, 30]. In that case, even though dynamics at $h \neq 0$ are chaotic, many quantities can be computed analytically, including various dynamical correlation functions. At these points, the IF has a perfect-dephaser form [25]. When parameters of the model are detuned slightly away from these PD points, the temporal entanglement remains low, showing an apparent volume-law scaling with T , albeit with a small prefactor; thus, the IF can be well-approximated by a MPS with a moderate bond dimension [25].

Here, we focus on the parameter choice $J = 0.8, g = 0.7236, h = 0.6472$, considered in Ref. [46]. It was found that such a model displays chaotic dynamics, and, moreover, the deviations from the eigenstate thermalization hypothesis quickly become negligible already at moderate finite sizes. We computed the IF for the infinite-temperature initial density matrix,

$$\rho_j^0 = \frac{1}{2} \begin{pmatrix} 1 & 0 \\ 0 & 1 \end{pmatrix} \quad (9)$$

by iteratively applying the dual transfer matrix to an initial “boundary” IF. As discussed below, certain choices of the boundary IF can significantly improve the performance of the MPS approach.

To perform the tensor network contraction, we set up a code using the tenpy library [47]. The diagonal form of interactions in the z -basis allows us to identify the input

and output legs at each time step (denoted by s and σ in Fig. 1). Thus, compared to the general circuits, the number of degrees of freedom in the dual transfer matrix and in the IM is reduced by a factor of 2 [25]; moreover, the maximum velocity of propagation is 1 rather than 2. The absence of correlations in the initial state of the chain combined with the strict light cone ensures that the IF reaches its self-consistent thermodynamic limit form after at most T iterations of the dual transfer matrix \tilde{T} . The latter can be straightforwardly represented as an MPO of bond dimension 4 for the model (8). We select a maximum bond dimension χ and iteratively apply this MPO to a boundary vector expressed in an MPS form, truncating the result to χ using SVD compression when necessary.

The choice of the boundary IF does not affect the final IF obtained after T iterations, provided the calculations are carried out exactly. However, different choices generally lead to different intermediate IFs encountered during iterations. Physically, the ℓ -th intermediate IF describes the effect of an environment that consists of ℓ spins, which evolve under unitary evolution set by the brick-wall quantum circuit, and are subject to an external bath at the boundary; the properties of this bath are determined by the chosen initial IF. In order for MPS-based methods to be efficient, it is important that the TE of the intermediate IF remains low enough, such that truncation does not incur a significant error. However, this is not always the case. Interestingly, seemingly the most natural choice of the boundary IF that corresponds to open boundary conditions, $\mathcal{I}[\sigma_\tau, \bar{\sigma}_\tau] = 1$, turns out not to be the most efficient one: in this case TE grows as a function of ℓ first before decreasing again to the final value. We found that the maximal TE entropy of intermediate IFs can be very high; its growth as a function of evolution time is shown by the dashed lines in

Fig. 2b. We note that a similar observation was reported in Ref. [26] for different models.

However, the problem of the “entanglement barrier” described above can be circumvented by choosing a different boundary IF. For the thermalizing Floquet model, we chose the perfect dephaser IF $I[\sigma_\tau, \bar{\sigma}_\tau] = \prod \delta_{\sigma_\tau, \bar{\sigma}_\tau}$ as a boundary condition. Physically, this corresponds to a boundary where the spin is measured (in the σ^z -basis) every period. We confirmed that this choice indeed leads to a monotonic growth of entanglement as a function of iteration number ℓ , and therefore the “entanglement barrier” can be avoided.

Using the MPS representation of the IF we computed the dynamical correlation function:

$$C_{zz}(t) = \langle \hat{\sigma}_0^z(t) \hat{\sigma}_0^z(0) \rangle. \quad (10)$$

The resulting exponential decay of this correlator, illustrated in Fig. 2a, is consistent with the scrambling of local quantum information expected in this chaotic system.

Fig. 2b shows the scaling of TE entropy (for a bipartition at $\tau = T/2$) with the evolution time computed with the MPS approach for three choices of the maximum bond dimension. The convergence of TE for different bond dimensions up to $T \approx 20$ indicates that the MPS form provides a good approximation to the exact IF. For times up to $T = 7$ this was verified by comparing the results to exact ones found with the standard sparse linear algebra library ARPACK (blue crosses in Fig. 2). TE entropy follows an apparent volume-law scaling in the accessible time interval. We note that at present it is unclear whether this scaling persists as $T \rightarrow \infty$.

B. Hamiltonian dynamics

We can use a related approach to study Hamiltonian dynamics, by viewing Eq. (8) as a (second-order) trotterization of the continuous time unitary flow $U = e^{-iHt}$ generated by the Hamiltonian

$$H = -J \sum_j \sigma_j^z \sigma_{j+1}^z - h \sum_j \sigma_j^z - g \sum_j \sigma_j^x. \quad (11)$$

This Hamiltonian describes a quantum Ising chain in a tilted magnetic field. The identification is realized by rescaling the parameters in the Hamiltonian Eq. (11) with the time step $0 < \epsilon \ll 1$ in order to obtain the dimensionless parameters $J, g, h \mapsto J\epsilon, g\epsilon, h\epsilon$ in Eq. (8); in this case, the physical time is $t = T\epsilon$. Higher-order Trotter schemes can be implemented analogously.

The model in Eq. (11), despite its apparent simplicity, exhibits a rich variety of phenomena, and therefore it provides a fruitful playground in quantum many-body physics, both in and out-of-equilibrium. Similarly to its Floquet counterpart, it is integrable when the magnetic field is purely transverse ($h = 0$), and exhibits a paradigmatic quantum phase transition between a paramagnetic

$|g| > J$ and a ferromagnetic $|g| < J$ phase, corresponding to a spontaneous breaking of the \mathbb{Z}_2 symmetry. The free fermionic quasiparticles of the model change their nature across the transition, from non-topological, spin-wave-like to topological, domain-wall-like excitations interpolating between the two degenerate vacua [48]. In the latter case, the longitudinal field h explicitly breaks the symmetry, lifting the degeneracy of the two magnetized ground states and inducing a first-order transition. Accordingly, a confining potential $V(r) \propto hr$ arises between a pair of domain walls, which bind together into “mesonic” composite particles [49]. The model with nonvanishing fields $g, h \neq 0$ is non-integrable and its dynamics are believed to be generally chaotic [46], although anomalously slow or even suppressed relaxation after a quench has been reported even far away from solvable limits [50–52] and related to confinement of excitations [36–39].

First, we study the local relaxation of a slower impurity spin at position $j = 0$ embedded in the quantum Ising chain at infinite temperature. This impurity is characterized by having smaller values of the fields $g_0 = \alpha g, h_0 = \alpha h$ and of the couplings $J_{-1,0} = J_{0,1} = \beta J$ to the neighboring spins. Note that the IF only depends on β and not on α . Tuning β and α to be much smaller than 1, the impurity dynamics approaches a typical open quantum system (OQS) setup, i.e., that of a two-level system weakly coupled to a much faster environment, which allows for the celebrated Born (for $\beta \ll 1$) and Markov (for $\alpha \ll 1$) approximations, respectively. Putting β and α to 1, instead, we retrieve the standard homogeneous quantum many-body system setup, where the distinction between the relevant subsystem and its bath is purely conceptual. Fig. 3 illustrates representative results of these computations. The left panel shows the infinite-temperature time-dependent autocorrelator $C_{zz}(t)$ [cf. Eq. (10)] converged with respect to both Trotter step and bond dimension, for decreasing α and β from the homogeneous case to an OQS limit. The right panel shows the scaling of TE entropy S converged with respect to the bond dimension vs the physical evolution time t (i.e., for $T = t/\epsilon$ steps), for a range of decreasing Trotter steps ϵ . Interestingly, for fixed t , the value of S scales to zero for $\epsilon \rightarrow 0$ with an apparent power law with an exponent $\simeq 1.8$. We will further comment on this observation below.

Second, we study a prototypical quantum quench setup, where the (now impurity-free) system is initialized in a fully polarized state in the positive z direction. We focus on the ferromagnetic phase, setting $g = 0.25J$ and $h = 0.4J$. The evolution of the ferromagnetic order parameter $\langle \sigma_0^z(t) \rangle$ in Fig. 4 displays clear, long-lived quasiperiodic oscillations, consistent with the discrete tower of mesonic particles excited by the sudden quench [36]. The right panel shows that the same scaling of the maximum TE entropy with the Trotter step is found even for quench dynamics, cf. Fig. 3. In this case, furthermore, it makes sense to compare spatial entan-

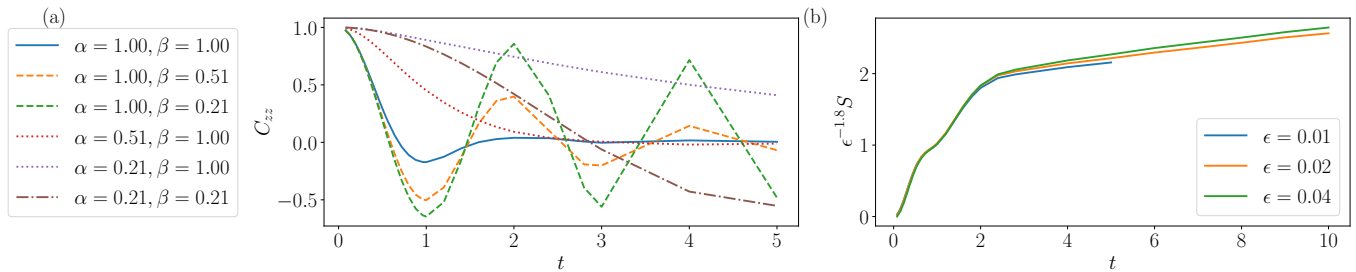


Figure 3. *Left*: Autocorrelation C_{zz} of Hamiltonian model (11) for parameters $J = 1.0, g = \sqrt{2}, h = 0.681$ at infinite temperature with different impurities. The parameters were chosen to be incommensurate to avoid any resonances which may affect dynamical properties. The result for a homogeneous chain is plotted by the solid line. We can observe the perturbative (Born) limit by tuning the coupling of the impurity spin to the spin chain (dotted lines) and the memoryless (Markovian) limit by tuning the driving of the impurity (dashed lines) as well as the combined Born-Markov limit (dash-dotted line). The calculation is fully converged for bond dimensions $\chi = 64, 128$ and time steps $\epsilon = 0.01, 0.02, 0.04$. *Right*: TE entropy scales to zero as a function of the time step ϵ , in a manner that is approximately consistent with a power-law dependence on ϵ in the parameter range considered.

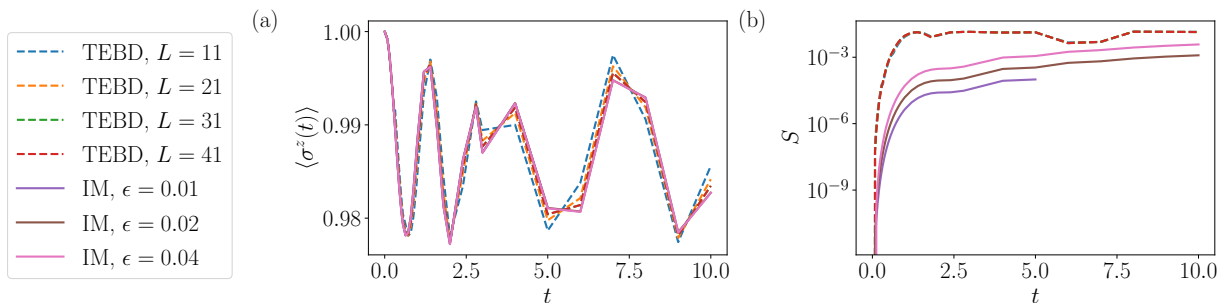


Figure 4. Comparison of TEBD and IM methods for the Hamiltonian model (11) at $J = 1.0, g = 0.25, h = 0.4$ undergoing a quench from the polarized state (cf Refs. [36, 50]). In both cases, bond dimension $\chi = 64$ was used. *Left*: While both curves are converged with respect to time step and bond dimension, the TEBD results still show small finite size effects. *Right*: The real space entanglement entropy of the TEBD MPS is significantly higher than the TE entropy for all three time steps, indicating the lower computational cost of the IM approach.

gument entropy to temporal entanglement entropy. As the plot clearly shows, the former – obtained by TEBD converged with system size and bond dimension – significantly exceeds the latter, while still remaining relatively low as a consequence of confinement [36, 39].

C. Continuous-time limit

The simulations presented in this Section were obtained with a second-order Trotter scheme with time steps $\epsilon = 0.01, 0.02, 0.04$. The Trotter error was found to be negligible in all cases for $\epsilon \leq 0.04$: in the examples shown in Figs. 3, 4, time-dependent observables were perfectly converged with respect to decreasing ϵ . Thus, effectively, the continuous time limit is well captured by the discretized evolution.

On the methodological side, it is interesting to discuss the non-trivial scaling of temporal entanglement when ϵ is decreased. Surprisingly, as shown in the right panel of Fig. 3, the maximum temporal entanglement entropy S_t at fixed physical evolution time t scales to zero for $\epsilon \rightarrow 0$. This behavior was found in all our simulations of

Hamiltonian dynamics. To gain an insight into the origin of this behavior, below we analyze several solvable limits.

First, we study the continuous-time limit of the IM in the limiting case $g = 0$, where quantum fluctuations are completely suppressed and all product states in the σ^z -basis are eigenstates of the Floquet operator/Hamiltonian for all J, h . Let us first consider the Floquet problem of Eq. (8), with an infinite-temperature initial ensemble. The analytical form of the IM can be found exactly:

$$I[\sigma_\tau, \bar{\sigma}_\tau] = \cos \left[J \sum_{\tau} (\sigma_\tau - \bar{\sigma}_\tau) \right]. \quad (12)$$

It is straightforward to verify that this expression satisfies the self-consistency equation for $g = 0$. Physically, this expression can be thought of as the influence functional due to an interaction with a constant classical magnetic field along \hat{z} -axis, which takes values $+J$ or $-J$ with probability $1/2$. To compute the von Neumann entropy of I , we need to normalize it as a pure wavefunction in the folded Hilbert space, i.e.,

$$|\Psi\rangle = \frac{1}{\sqrt{2[1 + \cos^{2T}(2J)]}} \left(\bigotimes_{\tau} \frac{1}{2} \begin{pmatrix} 1 \\ 1 \end{pmatrix}_{cl,\tau} \otimes \begin{pmatrix} e^{2iJ} \\ e^{-2iJ} \end{pmatrix}_{q,\tau} + \bigotimes_{\tau} \frac{1}{2} \begin{pmatrix} 1 \\ 1 \end{pmatrix}_{cl,\tau} \otimes \begin{pmatrix} e^{-2iJ} \\ e^{+2iJ} \end{pmatrix}_{q,\tau} \right) \quad (13)$$

where we have factored the four-dimensional folded Hilbert space at time τ into the tensor product of a “classical” $\text{Span}(|\uparrow\uparrow\rangle, |\downarrow\downarrow\rangle)$ and a “quantum” $\text{Span}(|\uparrow\downarrow\rangle, |\downarrow\uparrow\rangle)$ two-dimensional subsystems. The chosen prefactor ensures the normalization condition, $\langle\Psi|\Psi\rangle = 1$.

Our aim is to compute the bipartite von Neumann entanglement entropy of this normalized state wavefunction with respect to a bipartition $(1, M), (M + 1, T)$. First, we notice that the classical sector does not contribute to entanglement, since the corresponding degrees of freedom are in a product state. Second, restricted to the quantum sector, $|\Psi\rangle$ can be thought of as an equal-weight quantum superposition of two pure spin-coherent states of a spin of magnitude $T/2$, fully polarized along the directions $\cos(2J)\hat{x} \pm \sin(2J)\hat{y}$, respectively. These two spin-coherent states can be pictured as Gaussian wavepackets on the surface of the Bloch sphere, centered around those two directions, with transverse fluctuations of width equal to $1/\sqrt{T}$ (relative to the unit radius of the Bloch sphere). Since the two polarization directions form an angle $4J$, it is easy to see that the overlap of the two spin-coherent states decreases exponentially with J^2T . For $J^2T \ll 1$, the two states have large overlap, so $|\Psi\rangle$ is close to a product state, giving a vanishing von Neumann entanglement entropy. In contrast, for $J^2T \gg 1$, the two states are effectively orthogonal, such that $|\Psi\rangle$ becomes a GHZ state with von Neumann entanglement entropy $\log 2$. The exact calculation gives the binary entropy

$$S_{M,T}(J) = -P \log P - (1 - P) \log(1 - P), \quad (14)$$

with

$$P = 1 - \frac{\cos^{2M}(2J) + \cos^{2(T-M)}(2J)}{1 + \cos^{2T}(2J)}, \quad (15)$$

which exhibits the expected features. Setting $x = J^2T$, $0 \leq f = M/T \leq 1$, this quantity becomes a smooth function of x and f in the limit $T \rightarrow \infty$.

We are now in a position to understand the continuous-time limit in this solvable case. Setting $J = \epsilon$, $T = t/\epsilon$, we find that the variable $J^2T = \epsilon t$ flows to zero for any fixed value of the physical evolution time t . Since $P \sim \epsilon^2$ as $\epsilon \rightarrow 0$, the von Neumann entropy of any extensive bipartition converges to zero in the continuous-time limit. It is instructive to note that in this case the entanglement spectrum is composed of only two values, P and $1 - P$. When ϵ is sufficiently small, one might be tempted to truncate the corresponding singular value (e.g., when performing a standard SVD compression). This seemingly harmless approximation, however, would produce incorrect results. Indeed, after such a truncation, the IM becomes a product state relative to the considered bipartition, say at the bond $(M, M + 1)$: physically, this

corresponds to “refreshing the environment”, i.e., tracing it out after M time steps and replacing it with another infinite-temperature environment before time step $M + 1$. Performing a similar truncation in other bonds, we end up with an IM corresponding to a “noisy” classical magnetic field along \hat{z} switching between $\pm J$, whereas the actual exact IM in Eq. (12) represents the influence of a constant field. We thus conclude that in the continuous-time limit, truncation of small Schmidt values might be dangerous, and may not lead to an accurate representation of system’s dynamics. Furthermore, counter-intuitively, the mere value of temporal entropy is not representative of the extent of temporal correlations and of the computational resources needed to parametrize the IM.

We have further confirmed this picture by an analytical calculation of the IF in the integrable limit $\hbar = 0$ [40]. Making use of the quadratic fermionic representation of the model, S_t is reduced to the entropy of a Bardeen-Cooper-Schrieffer-like wavefunction on the Keldysh contour, due to its Gaussian form. In this case, as shown in Fig. 5, the scaling of S_t with ϵ stems from an ϵ^2 global scaling of the single-particle entanglement spectrum, $p_n \sim \epsilon^2 P_n$, which gives

$$S_{\tau,t} \equiv - \sum_n p_n \log p_n + (1 - p_n) \log(1 - p_n) \sim \epsilon^2 [\log(1/\epsilon^2) + \hat{S}], \quad (16)$$

where $\hat{S} = - \sum_n P_n \log P_n + (1 - P_n) \log(1 - P_n)$ is a finite, ϵ -independent quantity. Once again, our tentative conclusion that all the singular values could be safely truncated as $\epsilon \rightarrow 0$ would lead to an incorrect description of dynamics, as the resulting product-state form of the IM would be incompatible with the existence of finite temporal correlations in the continuous-time limit.

The behavior of the IM at $\epsilon \rightarrow 0$ in the solvable cases discussed above indicates that caution must be exercised when applying conventional compression techniques to influence functionals. Thus, in the future it would be beneficial to develop other numerical schemes that take into account the structural constraints of IMs in the continuous-time limit.

IV. NON-ERGODIC DYNAMICS: DISCRETE TIME CRYSTALS

The influence functional approach allows to treat the effects of spatially uncorrelated randomness via exact ensemble averaging, denoted by $\mathbb{E}(\cdot)$. As in the Schwinger-Keldysh path integral formalism [53], ensemble-averaged observables can be found from the ensemble-averaged IF,

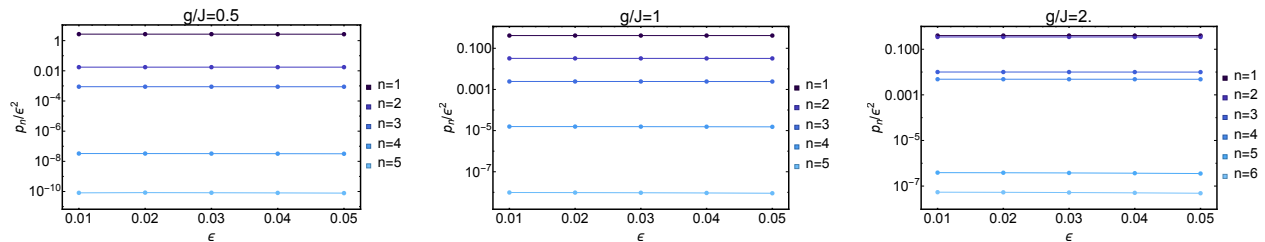


Figure 5. Behavior of the single-particle entanglement spectrum of the IM of the transverse-field quantum Ising chain. The largest eigenvalues $0 \leq p_n \leq 1/2$ of the correlation matrix of a half-time interval originating from the IM wavefunction $|\Psi\rangle$ (see the text) are reported, rescaled by ϵ^2 , as a function of ϵ , for three values of g/J reported above the plots. In all cases, the results indicate the scaling behavior $p_n \sim \epsilon^2 P_n$, where P_n are ϵ -independent quantities.

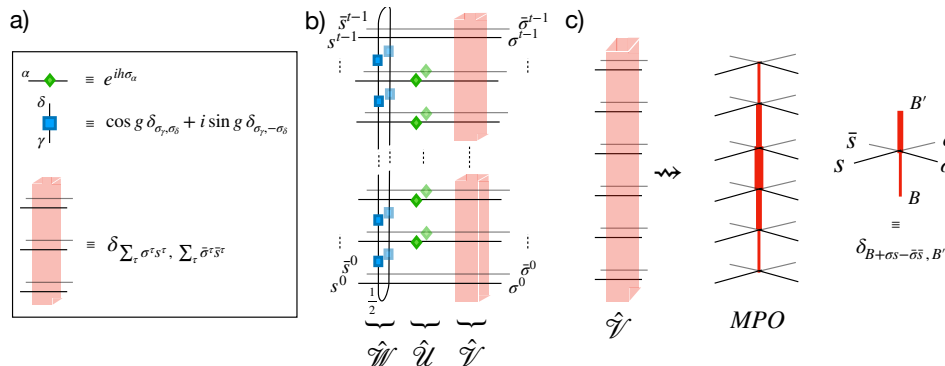


Figure 6. Depiction of the tensor network corresponding to the discrete path integral of the Floquet model with fully random J . Averaging over J can be implemented by an operator $\delta_{\sum_c s\sigma \sum_c \bar{s}\bar{\sigma}}$. This operator can be implemented as an MPO by introducing a virtual index which at each spin corresponds to the difference in partial sums up to this spin. The condition can be enforced by only allowing partial sum values that are consistent with it. The maximal bond dimension of the resulting operator is t .

without the need of introducing replicas. Provided randomness in different spatial points is uncorrelated (or short-range correlated), and provided its distribution is spatially homogeneous, the ensemble-averaged IF satisfies a self-consistency equation defined by the transfer matrix $\mathbb{E}(\hat{T})$. This applies to various kinds of randomness. Above we have already introduced ensemble-averaging over statistical mixtures of initial states (in particular, infinite-temperature density matrices). Random spatiotemporal noise can also be easily incorporated; in Ref. [25], we showed that circuits with fully random Haar-distributed kicks and fully random diagonal interactions behave as perfect dephasers (almost surely in the ensemble distribution in the limit of large local Hilbert space). Furthermore, in Ref. [33], the formalism was applied to systems with quenched disorder. In this case, the random variables are constant in time, and exact averaging over them introduces non-local in time effective interactions in the problem.

One of the most appealing aspects of the IF approach is that the self-consistent IF fully encodes the ability of a quantum many-body system to provide an efficient thermal bath. In particular, it should be possible to classify universality classes of quantum dynamics based on the structure of their IF, e.g., to distinguish between ergodicity vs non-ergodicity. It is known that strongly

disordered quantum lattice systems can break ergodicity via the mechanism of many-body localization (MBL) [9]. Reference [33] began to explore the MBL transition using the IF approach. The model considered in Ref. [33] is the kicked Ising chain of Eq. (8) with random longitudinal fields h_j uniformly distributed in $[0, 2\pi)$. This model exhibits a Floquet-MBL transition upon varying the relative strength of the transverse field and/or of interactions [54, 55].

Discrete time crystals (DTCs) represent a notable regime of non-equilibrium quantum dynamics. DTC behavior in periodically driven quantum lattice systems is associated with a robust spatiotemporal order that spontaneously breaks the discrete time-translation symmetry. A DTC phase requires a coherent periodic drive and an underlying physical mechanism protecting the system from indefinite heating, such as MBL or prethermalization [56, 57]. DTC response is robust against arbitrary (weak) perturbations of the system interactions and of the driving protocol [16, 17]. Below we show that the IM approach provides a suitable tool for this phenomenon as well. Indeed, the IM formalism naturally incorporates the necessary ingredients to observe time-crystalline behavior, namely discrete time-translation symmetry, thermodynamic limit, and disorder averaging.

DTC response can be observed, in particular, in a

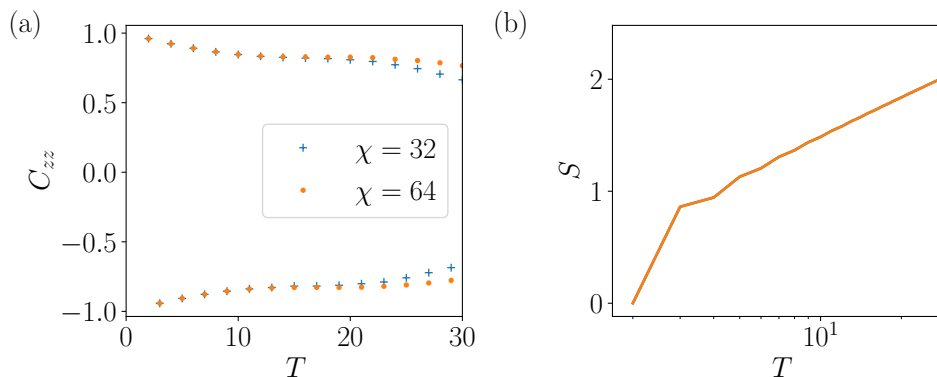


Figure 7. Discrete time crystal simulated using influence functional approach. We use a Floquet model in Eq. (17) with parameters $g = \frac{\pi}{2} - 0.1$, $h = 0.3$, and J fully random. The initial state corresponds to an infinite temperature ensemble. *Left*: C_{zz} correlations show persistent oscillations. For larger time, the amplitude of oscillations decreases for bond dimension $\chi = 32$, which is attributed to the effects of the compression. *Right*: TE grows logarithmically with evolution time. Two curves for different bond dimensions coincide.

kicked Ising model with random interactions and single-spin kicks close to perfect π -rotations around the \hat{x} axis [16, 17]. We consider the model in Eq. (8), introducing bond-dependent couplings J_j uniformly distributed in $[0, 2\pi]$, and setting $g = \pi/2 - \varepsilon$:

$$U = e^{-i(\pi/2-\varepsilon)\sum_j \sigma_j^x} e^{-\sum_j J_j \sigma_j^z \sigma_{j+1}^z - h \sum_j \sigma_j^z}. \quad (17)$$

For $\varepsilon = 0$, the kick commutes with the interaction term: every initial product state in the z -basis undergoes perfect flips of all the spins each period, and thus returns to the initial configuration every other driving period, exhibiting a trivial DTC dynamics. When ε is non-zero, but sufficiently small, the subharmonic DTC response of the system survives many-body quantum fluctuations. The robustness of the DTC is made possible by MBL, which prevents the domain-wall excitations generated by the periodic quenches from spreading across the chain and melting the spatiotemporally ordered pattern, as it would happen in the absence of disorder.

To analyze DTC behavior using the IF formalism, we first note that averaging over J in the dual transfer matrix can be done exactly:

$$\int \frac{dJ}{2\pi} \prod_{\tau} \exp [iJ(\sigma^{\tau} s^{\tau} - \bar{\sigma}^{\tau} \bar{s}^{\tau})] = \delta_{\sum_{\tau} \sigma^{\tau} s^{\tau}, \sum_{\tau} \bar{\sigma}^{\tau} \bar{s}^{\tau}}. \quad (18)$$

The resulting operator can be interpreted as an adjacency matrix, which allows a transition between trajectories $\sigma_{\tau}, \bar{\sigma}_{\tau}$ and s_{τ}, \bar{s}_{τ} as long as the total number of spins flipped on the forward trajectory is equal to the total number of spins flipped on the backward trajectory. We can express this operator as a MPO as depicted in Fig. 6: Each tensor in the MPO is given by $\delta_{B+\sigma^{\tau} s^{\tau} - \bar{\sigma}^{\tau} \bar{s}^{\tau}, B'}$ where the virtual indices B, B' carry the running sums of flipped spins on the forward minus those on the backward trajectory, such that the averaging condition (18) is globally enforced. This procedure yields an MPO with bond dimension t . Since bond dimension

of the operator is relatively large, we cannot apply the MPO to the MPS and compress the result. Instead, the compression needs to happen during the application of the operator [58].

To detect subharmonic response, we computed the (disorder-averaged) IM using an MPO-based algorithm, and used it to calculate the dynamical correlation function $C_{zz}(T)$. The model (17), similar to closely related models considered in Refs. [16, 17], exhibits a DTC phase at sufficiently small detuning from a perfect π -rotation, ε . This is evident in Fig. 7, which illustrates $C_{zz}(T)$ for $\varepsilon = 0.1, h = 0.3$. The correlator exhibits persistent oscillations with an amplitude that stays sizeable at the times simulated. Note the slight decay at times $T > 20$ for the smaller bond dimension; we attribute it to the errors introduced by compression to an MPS form. Indeed, increasing the bond dimension χ restores the stable oscillatory behavior for longer times. We have further observed that for $\varepsilon \gtrsim 0.3$ the behavior changes qualitatively, and the correlation function decays at short, χ -independent time scales, suggesting that the system enters a thermalizing phase.

To assess the efficiency of the method, we have also analyzed the scaling of TE entropy with T (right panel of Fig. 7, converged with respect to χ), finding it to be approximately logarithmic. To understand the origin of this behavior, let us consider the trivial DTC point $\varepsilon = 0$, i.e., $g = \pi/2$. In this case quantum fluctuations are completely suppressed, and, analogously to Eq. (11), the exact IM for spin j reads

$$I[\sigma_{\tau}, \bar{\sigma}_{\tau}] = \cos [J_j \sum_{\tau} (-)^{\tau} (\sigma_{\tau} - \bar{\sigma}_{\tau})]. \quad (19)$$

Taking the exact average over the random coupling J_j , we obtain

$$\mathbb{E}(I[\sigma_{\tau}, \bar{\sigma}_{\tau}]) = \delta_{\sum_{\tau} (-)^{\tau} \sigma_{\tau}, \sum_{\tau} (-)^{\tau} \bar{\sigma}_{\tau}}. \quad (20)$$

Viewed as a wavefunction in the folded multi-time Hilbert space, similarly to what done in Eq. (12), we find that

$$\mathbb{E}(I[\sigma_\tau, \bar{\sigma}_\tau]) \mapsto \Psi = \left(\bigotimes_\tau \frac{1}{\sqrt{2}} \begin{pmatrix} 1 \\ 1 \end{pmatrix}_{cl,\tau} \right) \otimes \left| \frac{T}{2}, 0 \right\rangle_q \quad (21)$$

where $|\frac{T}{2}, 0\rangle_q$ represents the Dicke state of T spins-1/2 with *staggered* collective spin magnitude $S = \frac{T}{2}$ and magnetization $S_z = 0$. The entanglement entropy of this wavefunction scales as $\frac{1}{2} \log T$. This form of temporal entanglement stems from the effective long-range interactions in time arising from exact disorder averaging. (We observe that a similar conclusion applies to the case $g = 0$, where the collective spin magnetization is uniform rather than staggered.)

We finally note that Ref. [33], which considered Floquet-MBL phase in a random- h kicked Ising model, found that the scaling of TE entropy was strongly sub-linear in the MBL phase, qualitatively similar to what is reported above. However, we note that there a variational DMRG approach to computing the IM was used, while here we employed iterative algorithm. In the future, it would be interesting to compare the performance of the two approaches to solving self-consistency equation for different models.

V. SUMMARY AND OUTLOOK

In this paper, we characterized dynamics of a many-body system via its influence functional – an object commonly used for describing dynamics of open quantum systems. IF provides a tool for quantifying the ability (or lack thereof) of a many-body systems to serve as a thermal bath for its parts [25, 33]. One of our goals was to illustrate the versatility of this new approach, by applying it to describe dynamics in very different regimes and setups. In particular, we studied thermalization in chaotic Floquet and Hamiltonian models, as well as its absence, accompanying the DTC response, in disordered systems.

A central role in our analysis was played by the temporal entanglement of the IF “wavefunction”, which is an analogue of the conventional real-space entanglement of many-body wavefunctions. Similarly to the case of ground states in many-body systems, temporal entanglement serves as a measure of the computational complexity of parametrizing the IF by a MPS. As discussed above, in several physical situations of interest, temporal entan-

glement remains low, providing new corners where many-body dynamics can be efficiently simulated (and, in some cases even solvable). Furthermore, we expect that other measures of temporal entanglement of IF could provide a witness of universal aspects of dynamics, for example, distinguishing between ergodic and non-ergodic dynamics.

Looking forward, the IF formalism appears suitable for studying entanglement transitions in hybrid quantum circuits composed of unitary gates and projective measurements or local dissipation [59, 60]: indeed, both randomness and dissipation can be naturally incorporated in this approach. We expect that the character of the asymptotic state of such systems is encoded in the structure of the self-consistent, ensemble-averaged influence matrix. On a more practical level, the development of efficient numerical schemes to approximate the IF of generic quantum many-body systems, while challenging, is a promising direction for future research, which may provide new insights into several long-standing problems in quantum dynamics, including the nature of the MBL-thermal transition [61–66].

Finally, we hope that the approach outlined above will stimulate new fruitful connections between theory of open quantum systems and quantum many-body dynamics [26, 34, 35]. For example, one can envision that standard concepts of the former – such as memory kernels [67] and non-Markovianity measures [68] – may be turned into new tools for the latter. Progress in this direction may enable classification of universal basins of attraction in quantum many-body dynamics. In addition, ideas and tools from quantum many-body physics, including tensor-networks, could widen the scope of open quantum systems theory, for example, allowing one to describe the effects of truly interacting, quantum chaotic environments.

VI. ACKNOWLEDGMENTS

This work was supported by the Swiss National Science Foundation and by the European Research Council (ERC) under the European Union’s Horizon 2020 research and innovation programme (grant agreement No. 864597). We thank Lorenzo Piroli and Soonwon Choi for useful discussions. Computations were performed at the University of Geneva on the “Baobab” and “Yggdrasil” HPC clusters.

-
- [1] H.-P. Breuer and F. Petruccione, *The theory of open quantum systems* (Oxford University Press, 2007).
 [2] Ulrich Weiss, *Quantum Dissipative Systems*, 4th ed. (WORLD SCIENTIFIC, 2012) <https://www.worldscientific.com/doi/pdf/10.1142/8334>.

- [3] R.P Feynman and F.L Vernon, “The theory of a general quantum system interacting with a linear dissipative system,” *Annals of Physics* **24**, 118 – 173 (1963).
 [4] A. J. Leggett, S. Chakravarty, A. T. Dorsey, Matthew P. A. Fisher, Anupam Garg, and W. Zwerger, “Dynamics

- of the dissipative two-state system,” *Rev. Mod. Phys.* **59**, 1–85 (1987).
- [5] Immanuel Bloch, Jean Dalibard, and Wilhelm Zwerger, “Many-body physics with ultracold gases,” *Rev. Mod. Phys.* **80**, 885–964 (2008).
- [6] R. Blatt and C. F. Roos, “Quantum simulations with trapped ions,” *Nature Physics* **8**, 277–284 (2012).
- [7] Luca D’Alessio, Yariv Kafri, Anatoli Polkovnikov, and Marcos Rigol, “From quantum chaos and eigenstate thermalization to statistical mechanics and thermodynamics,” *Advances in Physics* **65**, 239–362 (2016).
- [8] Rahul Nandkishore and David A. Huse, “Many-body localization and thermalization in quantum statistical mechanics,” *Annual Review of Condensed Matter Physics* **6**, 15–38 (2015).
- [9] Dmitry A. Abanin, Ehud Altman, Immanuel Bloch, and Maksym Serbyn, “Colloquium: Many-body localization, thermalization, and entanglement,” *Rev. Mod. Phys.* **91**, 021001 (2019).
- [10] Fabien Alet and Nicolas Laflorencie, “Many-body localization: An introduction and selected topics,” *Comptes Rendus Physique* **19**, 498 – 525 (2018).
- [11] P. W. Anderson, “Absence of diffusion in certain random lattices,” *Phys. Rev.* **109**, 1492–1505 (1958).
- [12] Pedro Ponte, Z. Papić, François Huveneers, and Dmitry A. Abanin, “Many-body localization in periodically driven systems,” *Phys. Rev. Lett.* **114**, 140401 (2015).
- [13] Achilleas Lazarides, Arnab Das, and Roderich Moessner, “Fate of many-body localization under periodic driving,” *Phys. Rev. Lett.* **115**, 030402 (2015).
- [14] Dmitry A. Abanin, Wojciech De Roeck, and François Huveneers, “Theory of many-body localization in periodically driven systems,” *Annals of Physics* **372**, 1 – 11 (2016).
- [15] Pranjal Bordia, Henrik Lüschen, Ulrich Schneider, Michael Knap, and Immanuel Bloch, “Periodically driving a many-body localized quantum system,” *Nature Physics* **13**, 460–464 (2017).
- [16] Vedika Khemani, Achilleas Lazarides, Roderich Moessner, and S. L. Sondhi, “Phase structure of driven quantum systems,” *Phys. Rev. Lett.* **116**, 250401 (2016).
- [17] Dominic V. Else, Bela Bauer, and Chetan Nayak, “Floquet time crystals,” *Phys. Rev. Lett.* **117**, 090402 (2016).
- [18] Frederik Nathan, Dmitry Abanin, Erez Berg, Netanel H. Lindner, and Mark S. Rudner, “Anomalous floquet insulators,” *Phys. Rev. B* **99**, 195133 (2019).
- [19] Fabian H L Essler and Maurizio Fagotti, “Quench dynamics and relaxation in isolated integrable quantum spin chains,” *Journal of Statistical Mechanics: Theory and Experiment* **2016**, 064002 (2016).
- [20] Maksym Serbyn, Dmitry A. Abanin, and Zlatko Papić, “Quantum Many-Body Scars and Weak Breaking of Ergodicity,” arXiv e-prints , arXiv:2011.09486 (2020), arXiv:2011.09486 [quant-ph].
- [21] J. M. Deutsch, “Quantum statistical mechanics in a closed system,” *Phys. Rev. A* **43**, 2046–2049 (1991).
- [22] Mark Srednicki, “Chaos and quantum thermalization,” *Phys. Rev. E* **50**, 888–901 (1994).
- [23] F. Verstraete, V. Murg, and J.I. Cirac, “Matrix product states, projected entangled pair states, and variational renormalization group methods for quantum spin systems,” *Advances in Physics* **57**, 143–224 (2008).
- [24] Sebastian Paeckel, Thomas Köhler, Andreas Swoboda, Salvatore R. Manmana, Ulrich Schollwöck, and Claudius Hubig, “Time-evolution methods for matrix-product states,” *Annals of Physics* **411**, 167998 (2019).
- [25] Alessio Lerose, Michael Sonner, and Dmitry A. Abanin, “Influence matrix approach to many-body floquet dynamics,” (2021), arXiv:2009.10105 [cond-mat.str-el].
- [26] Erika Ye and Garnet Kin-Lic Chan, “Constructing Tensor Network Influence Functionals for General Quantum Dynamics,” arXiv e-prints , arXiv:2101.05466 (2021), arXiv:2101.05466 [quant-ph].
- [27] M. C. Bañuls, M. B. Hastings, F. Verstraete, and J. I. Cirac, “Matrix product states for dynamical simulation of infinite chains,” *Phys. Rev. Lett.* **102**, 240603 (2009).
- [28] Alexander Müller-Hermes, J Ignacio Cirac, and Mari Carmen Banuls, “Tensor network techniques for the computation of dynamical observables in one-dimensional quantum spin systems,” *New Journal of Physics* **14**, 075003 (2012).
- [29] M Akila, D Waltner, B Gutkin, and T Guhr, “Particle-time duality in the kicked ising spin chain,” *Journal of Physics A: Mathematical and Theoretical* **49**, 375101 (2016).
- [30] Bruno Bertini, Pavel Kos, and Tomaž Prosen, “Exact correlation functions for dual-unitary lattice models in 1 + 1 dimensions,” *Phys. Rev. Lett.* **123**, 210601 (2019).
- [31] Lorenzo Piroli, Bruno Bertini, J. Ignacio Cirac, and Tomaž Prosen, “Exact dynamics in dual-unitary quantum circuits,” *Phys. Rev. B* **101**, 094304 (2020).
- [32] Katja Klobas, Bruno Bertini, and Lorenzo Piroli, “Exact thermalization dynamics in the “Rule 54” Quantum Cellular Automaton,” arXiv e-prints , arXiv:2012.12256 (2020), arXiv:2012.12256 [cond-mat.stat-mech].
- [33] Michael Sonner, Alessio Lerose, and Dmitry A. Abanin, “Characterizing many-body localization via exact disorder-averaged quantum noise,” arXiv e-prints , arXiv:2012.00777 (2020), arXiv:2012.00777 [cond-mat.dis-nn].
- [34] A. Strathearn, P. Kirton, D. Kilda, J. Keeling, and B. W. Lovett, “Efficient non-Markovian quantum dynamics using time-evolving matrix product operators,” *Nature Communications* **9**, 3322 (2018).
- [35] Moritz Cygorek, Michael Cosacchi, Alexei Vagov, Vollrath Martin Axt, Brendon W. Lovett, Jonathan Keeling, and Erik M. Gauger, “Numerically-exact simulations of arbitrary open quantum systems using automated compression of environments,” arXiv e-prints , arXiv:2101.01653 (2021), arXiv:2101.01653 [quant-ph].
- [36] M. Kormos, M. Collura, G. Takács, and P. Calabrese, “Real time confinement following a quantum quench to a non-integrable model,” *Nature Physics* **13**, 246–249 (2017).
- [37] Andrew J. A. James, Robert M. Konik, and Neil J. Robinson, “Nonthermal states arising from confinement in one and two dimensions,” *Phys. Rev. Lett.* **122**, 130603 (2019).
- [38] Paolo Pietro Mazza, Gabriele Perfetto, Alessio Lerose, Mario Collura, and Andrea Gambassi, “Suppression of transport in nondisordered quantum spin chains due to confined excitations,” *Phys. Rev. B* **99**, 180302 (2019).
- [39] Alessio Lerose, Federica M. Surace, Paolo P. Mazza, Gabriele Perfetto, Mario Collura, and Andrea Gambassi, “Quasilocalized dynamics from confinement of quantum excitations,” *Phys. Rev. B* **102**, 041118 (2020).

- [40] Alessio Lerose, Michael Sonner, and Dmitry A. Abanin, “to appear,” arXiv e-prints (2021).
- [41] Christoph Sündershauf, David Pérez-García, David A. Huse, Norbert Schuch, and J. Ignacio Cirac, “Localization with random time-periodic quantum circuits,” *Phys. Rev. B* **98**, 134204 (2018).
- [42] Amos Chan, Andrea De Luca, and J. T. Chalker, “Spectral lyapunov exponents in chaotic and localized many-body quantum systems,” (2020), [arXiv:2012.05295 \[cond-mat.stat-mech\]](https://arxiv.org/abs/2012.05295).
- [43] S. J. Garratt and J. T. Chalker, “Many-body delocalization as symmetry breaking,” (2020), [arXiv:2012.11580 \[cond-mat.stat-mech\]](https://arxiv.org/abs/2012.11580).
- [44] Jutho Haegeman and Frank Verstraete, “Diagonalizing transfer matrices and matrix product operators: A medley of exact and computational methods,” *Annual Review of Condensed Matter Physics* **8**, 355–406 (2017), <https://doi.org/10.1146/annurev-conmatphys-031016-025507>.
- [45] M. B. Hastings and R. Mahajan, “Connecting entanglement in time and space: Improving the folding algorithm,” *Phys. Rev. A* **91**, 032306 (2015).
- [46] Hyungwon Kim, Tatsuhiko N. Ikeda, and David A. Huse, “Testing whether all eigenstates obey the eigenstate thermalization hypothesis,” *Phys. Rev. E* **90**, 052105 (2014).
- [47] Johannes Hauschild and Frank Pollmann, “Efficient numerical simulations with Tensor Networks: Tensor Network Python (TeNPy),” *SciPost Phys. Lect. Notes* **5** (2018), [10.21468/SciPostPhysLectNotes.5](https://doi.org/10.21468/SciPostPhysLectNotes.5), code available from <https://github.com/tenpy/tenpy>, [arXiv:1805.00055](https://arxiv.org/abs/1805.00055).
- [48] S. Sachdev, *Quantum Phase Transitions* (Cambridge University Press, 2011).
- [49] Barry M. McCoy and Tai Tsun Wu, “Two-dimensional ising field theory in a magnetic field: Breakup of the cut in the two-point function,” *Phys. Rev. D* **18**, 1259–1267 (1978).
- [50] M. C. Bañuls, J. I. Cirac, and M. B. Hastings, “Strong and weak thermalization of infinite nonintegrable quantum systems,” *Phys. Rev. Lett.* **106**, 050405 (2011).
- [51] Cheng-Ju Lin and Olexei I. Motrunich, “Quasiparticle explanation of the weak-thermalization regime under quench in a nonintegrable quantum spin chain,” *Phys. Rev. A* **95**, 023621 (2017).
- [52] Jonathan Wurtz and Anatoli Polkovnikov, “Emergent conservation laws and nonthermal states in the mixed-field ising model,” *Phys. Rev. B* **101**, 195138 (2020).
- [53] A. Kamenev, *Field Theory of Non-Equilibrium Systems* (Cambridge University Press, 2011).
- [54] Liangsheng Zhang, Vedika Khemani, and David A. Huse, “A floquet model for the many-body localization transition,” *Phys. Rev. B* **94**, 224202 (2016).
- [55] Michael Sonner, Maksym Serbyn, Zlatko Papić, and Dmitry A. Abanin, “Thouless energy in a floquet model of many-body localization,” (2020), [to appear](https://arxiv.org/abs/2012.05295).
- [56] Dmitry A. Abanin, Wojciech De Roeck, Wen Wei Ho, and François Huetteners, “Effective hamiltonians, prethermalization, and slow energy absorption in periodically driven many-body systems,” *Phys. Rev. B* **95**, 014112 (2017).
- [57] Dominic V. Else, Bela Bauer, and Chetan Nayak, “Prethermal phases of matter protected by time-translation symmetry,” *Phys. Rev. X* **7**, 011026 (2017).
- [58] E M Stoudenmire and Steven R White, “Minimally entangled typical thermal state algorithms,” *New Journal of Physics* **12**, 055026 (2010).
- [59] Brian Skinner, Jonathan Ruhman, and Adam Nahum, “Measurement-induced phase transitions in the dynamics of entanglement,” *Phys. Rev. X* **9**, 031009 (2019).
- [60] Yaodong Li, Xiao Chen, and Matthew P. A. Fisher, “Measurement-driven entanglement transition in hybrid quantum circuits,” *Phys. Rev. B* **100**, 134306 (2019).
- [61] Andrew C. Potter, Romain Vasseur, and S. A. Parameswaran, “Universal properties of many-body delocalization transitions,” *Phys. Rev. X* **5**, 031033 (2015).
- [62] Ronen Vosk, David A. Huse, and Ehud Altman, “Theory of the many-body localization transition in one-dimensional systems,” *Phys. Rev. X* **5**, 031032 (2015).
- [63] Liangsheng Zhang, Bo Zhao, Trithep Devakul, and David A. Huse, “Many-body localization phase transition: A simplified strong-randomness approximate renormalization group,” *Phys. Rev. B* **93**, 224201 (2016).
- [64] Philipp T. Dumitrescu, Romain Vasseur, and Andrew C. Potter, “Scaling theory of entanglement at the many-body localization transition,” *Phys. Rev. Lett.* **119**, 110604 (2017).
- [65] Thimothée Thiery, François Huetteners, Markus Müller, and Wojciech De Roeck, “Many-body delocalization as a quantum avalanche,” *Phys. Rev. Lett.* **121**, 140601 (2018).
- [66] Anna Goremykina, Romain Vasseur, and Maksym Serbyn, “Analytically solvable renormalization group for the many-body localization transition,” *Phys. Rev. Lett.* **122**, 040601 (2019).
- [67] Dmitrii E. Makarov and Nancy Makri, “Path integrals for dissipative systems by tensor multiplication. Condensed phase quantum dynamics for arbitrarily long time,” *Chemical Physics Letters* **221**, 482–491 (1994).
- [68] Heinz-Peter Breuer, Elsi-Mari Laine, Jyrki Piilo, and Bassano Vacchini, “Colloquium: Non-markovian dynamics in open quantum systems,” *Rev. Mod. Phys.* **88**, 021002 (2016).